Water-assisted generation of catalytic interface

The case of interfacial Pt-$FeO_x(OH)_y$ sites active in preferential carbon monoxide oxidation

Sadykov, Ilia I.; Palagin, Dennis; Krumeich, Frank; Plokhikh, Igor V.; van Bokhoven, Jeroen A.; Nachtegaal, Maarten; Safonova, Olga V.

DOI
10.1016/j.jcat.2023.115263

Publication date
2024

Document Version
Final published version

Published in
Journal of Catalysis

Journal of Catalysis 429 (2024) 115263

Contents lists available at ScienceDirect

Journal of Catalysis

journal homepage: www.elsevier.com/locate/jcat

Research article

Water-assisted generation of catalytic interface: The case of interfacial Pt-$FeO_x(OH)_y$ sites active in preferential carbon monoxide oxidation

Ilia I. Sadykov [a,b], Dennis Palagin [c], Frank Krumeich [b], Igor V. Plokhikh [a], Jeroen A. van Bokhoven [b,a], Maarten Nachtegaal [a], Olga V. Safonova [a,*]

[a] Paul Scherrer Institute, CH-5232 Villigen PSI, Switzerland
[b] ETH Zurich, Institute for Chemical and Bioengineering, CH-8093 Zurich, Switzerland
[c] Delft High Performance Computing Centre, Delft University of Technology, Mekelweg 4, 2628 CD Delft, The Netherlands

ARTICLE INFO

Keywords:
Preferential CO oxidation
Pt-Fe
Catalytic interface
Role of water
Structure-activity relationship
Operando
X-ray absorption spectroscopy
Infrared spectroscopy

ABSTRACT

The surface of supported heterogeneous catalysts often contains adsorbed water and hydroxyl groups even when water is not directly added to the reaction stream. Nonetheless, the reactivity of adsorbed water and hydroxyl groups is rarely considered. We demonstrate that water and hydroxyl groups can not only directly participate in the catalytic oxidation processes but are also able to generate and stabilize the catalytically active metal-oxide interface. We show that the reduction of Pt-Fe-supported catalysts with hydrogen in the presence of adsorbed water or steam allows for achieving one of the highest preferential carbon monoxide oxidation activities at ambient temperature. These conditions create active iron-associated hydroxyl groups next to platinum nanoparticles with enhanced reactivity towards carbon monoxide oxidation. Density functional theory calculations suggest that hydroxylation of oxidic iron species stabilizes the $FeO_x(OH)_y$/Pt interface, via strong metal-support interaction, which is confirmed by chemisorption measurements. Kinetic experiments, including those with ^{18}O-labeled water, in combination with operando infrared spectroscopy, show that water and hydroxyl groups directly participate in preferential carbon monoxide oxidation. A quantitative correlation between the catalytic activity of Pt-$FeO_x(OH)_y$/γ-Al_2O_3 catalysts and the Fe^{2+} concentration, obtained using operando X-ray absorption spectroscopy, shows that the number of active Fe^{2+} sites and the carbon monoxide oxidation rate per active site can be significantly increased by water-assisted pretreatment with hydrogen. This work provides a new example of positive role of strong metal-support interaction for the design of more active catalysts.

1. Introduction

Supported heterogeneous catalysts often operate in the presence of water and hydroxyl groups on the surface. Water is commonly present in the industrial gas streams and is also generated in situ, as a product, e.g. during carbon monoxide and carbon dioxide hydrogenation including Fischer-Tropsch synthesis and methanol production, etc. [1,2] Water potentially affects the structure of oxidic supports and supported phases, including metallic nanoparticles and highly dispersed oxides.

Relative humidity determines the coverage and the structure of adsorbed water on the surfaces of oxidic supports, as well as the concentration of hydroxyl groups [3–5]. Relative humidity above 70 % can lead to a formation of several layers of water together with the complex network of hydroxyl groups, which forms on oxidic supports even at a relative humidity below 10 % [6,7]. Non-reducible supports (e.g. Al_2O_3, SiO_2, zeolites) form hydroxyl groups upon interaction with water, which often plays a critical role in catalytic reactions [3–5]. Transition metal oxides (Fe_2O_3,FeO, CeO_2, ZnO, NiO) are known to form stable surface hydroxyls, when treated with water, which was demonstrated for single crystal surfaces using atomic force microscopy, infrared spectroscopy, and other methods [8–13].

Water-assisted treatments at high temperatures can lead to the

Abbreviations: PROX, preferential carbon monoxide oxidation; XAS, X-ray absorption spectroscopy; MS, mass spectrometer; TPR, temperature-programmed reduction; EXAFS, extended X-ray absorption fine structure; HAADF-STEM, high-angle annular dark-field scanning transmission electron microscopy; STEM, scanning transmission electron microscopy; XANES, X-ray absorption near-edge structure; DRIFTS, diffuse reflectance infrared Fourier transform spectroscopy; vol. %, volumetric percentage; TPD, temperature-programmed desorption.

* Corresponding author.
E-mail address: olga.safonova@psi.ch (O.V. Safonova).

https://doi.org/10.1016/j.jcat.2023.115263
Received 11 September 2023; Received in revised form 4 December 2023; Accepted 15 December 2023
Available online 21 December 2023

restructuring of supported metal nanoparticles [14,15,3,4]. Strong metal-support interaction manifested as stabilization and encapsulation of metal nanoparticles on reducible oxidic supports can also be influenced by water [16–18]. In some cases, this metal-support interaction leads to the nanoparticles growth or to changes in the size distribution, as it was shown for Pt/CeO_2 [19]. At the same time, another study demonstrated that the blockage of surface oxygen vacancies on TiO_2 by water hinders any restructuring of supported Pt nanoparticles even at 873 K [20]. The influence of water on the structure of metal-support interfaces therefore depends significantly on the nature of the system and is not properly studied.

Most detailed analysis of the effect of water on the catalytically active metal-oxide interface was done for the model Pt/FeO_x interfaces using atomic force microscopy, photoelectron spectroscopy and other surface science methods at low pressures. Fundamental studies performed with FeO(1 1 1) and Fe_3O_4(1 1 1) islands on the Pt(1 1 1) surface showed that water readily adsorbs on iron sites located at the FeO_x/Pt (1 1 1) interface and spontaneously dissociates to form iron-bound hydroxyl groups, which can migrate across FeO_x islands [8–10]. Hydrogen can also hydroxylate surface FeO_x species on Pt(1 1 1) through hydrogen spillover [21]. The obtained $FeO_x(OH)_y$ model layers are able to react with carbon monoxide adsorbed on Pt(1 1 1) already at 300 K [22]. However, there are no direct proofs of the involvement of water or hydroxyl groups in the reactivity of oxygen and carbon monoxide for the classical supported Pt-Fe catalysts operating at ambient pressure.

At the same time, such classical Pt-Fe catalysts, containing platinum nanoparticles and partially reduced FeO_x surface species supported on silica or alumina, demonstrate record activities in preferential carbon monoxide oxidation (PROX) at ambient temperature [1,2]. This process is considered a reasonable alternative to the inefficient methanation reaction used for reducing the carbon monoxide content in industrial hydrogen streams down to 100 ppm level. PROX is needed to prevent poisoning of the catalytic materials used in fuel cells operating at ambient temperatures and catalysts employed in ammonia synthesis process [1,2].

As water supplied in PROX feed or generated in situ during hydrogen oxidation does not evaporate below 373 K, it accumulates on the surface of ambient-temperature-active Pt-FeO_x catalysts and can affect carbon monoxide conversion and selectivity [23,24]. There is no distinct way of predicting if water is beneficial for Pt-FeO_x catalysts, as it can potentially affect both platinum and iron sites, and there is no clear consensus on its mechanism of action. Previous studies showed that supported Pt/FeO_x catalysts have higher activity for carbon monoxide oxidation when treated with water vapor [24,25]. At the same time, 20 % of added water poisoned Pt-Fe/mordenite and Pt-Fe/CNT (carbon nanotubes) catalysts [28,29]. As we have shown in our previous work, ambient temperature active Pt-Fe catalysts under PROX conditions contain active oxidic Fe^{2+} sites in contact with metallic Pt nanoparticles, which represent less than 20 % of all iron species [26]. However, we have not analyzed the influence of water on these sites. Other infrared and X-ray absorption spectroscopy studies also only analyzed how water affects the structure of the majority of iron and platinum species but did not reveal how water can affect the structure of the catalytically active sites [24–26].

In this work, we ventured to study how water affects not the entirety of supported Pt-$FeO_x(OH)_y$ catalysts but the actual active sites and the strong metal-support interaction between metallic platinum nanoparticles and iron oxidic species [17]. In particular, we focused on two questions: i) how does water affect the generation of active sites during water-assisted pretreatments in hydrogen at high temperatures and ii) how can water be involved in the reactivity of these sites during PROX reaction at ambient temperatures. These questions were tackled by operando X-ray absorption spectroscopy (XAS) complemented by operando diffuse reflectance infrared Fourier transform spectroscopy (DRIFTS), both following the state of the active species in real-time, as well as conversion and selectivity in real-time. These methods, together with ex situ scanning transmission electron microscopy (STEM), chemisorption measurements, kinetic characterization, and isotope-labeling experiments, showed how water treatment of supported Pt-Fe/γ-Al_2O_3 catalysts during the initial reduction step enables to create one of the most active PROX catalysts reported to date. In particular, we demonstrated that water-assisted treatments could promote partial encapsulation of platinum nanoparticles, generating and stabilizing highly PROX-active Fe^{2+} sites at the $FeO_x(OH)_y$/Pt interface. Moreover, we showed that hydroxyl groups on active $FeO_x(OH)_y$ islands can directly participate in carbon monoxide oxidation, promoting this reaction.

2. Results and discussion

2.1. Water-assisted pretreatment strategies

Synthesis of supported Pt-Fe catalysts and monometallic (Pt or Fe) reference samples was carried out by incipient wetness impregnation of corresponding porous γ-Al_2O_3 and SiO_2 supports. The impregnated supports were dried and then sequentially calcined in air for 2 h at 473 K and 2 h at 673 K. The samples obtained in this way were used in all subsequent experiments. Inductively coupled plasma-optical emission spectrometry (ICP-OES) determined the composition of the bimetallic samples to be 2.1 wt% Pt − 3.6 wt% Fe / γ-Al_2O_3 and 2.0 wt% Pt − 1.4 wt% Fe / SiO_2. Compositions of monometallic references were determined to be 2.0 wt% Pt / SiO_2, 2.0 wt% Pt / γ-Al_2O_3, and 3.4 wt% Fe / γ-Al_2O_3.

Reduction of such calcined samples under a hydrogen atmosphere is necessary to create active preferential carbon monoxide oxidation catalysts containing metallic platinum nanoparticles decorated with active oxidic Fe^{2+} species. As we found in our previous work, hydrogen pressure during reduction, as well as temperature, affect the degree of iron reduction [26,27]. Low reduction temperatures of 373–473 K are necessary to keep adsorbed water or hydroxyl groups on the surface and to avoid the formation of inactive metallic iron; which forms above 473 K [24–26]. Based on this, we have chosen pretreatment temperatures in the range of 373–473 K.

Four different pretreatment strategies were chosen to study the effect of water on the activity and the structure of the catalysts, as shown in **Fig. 1a** and **Table S1**. The first set of samples was reduced under pure hydrogen without added water. These materials are labelled as $Pt_{2.1}Fe_{3.6}$-Al_2O_3-473–100 and $Pt_{2.0}Fe_{1.4}$-SiO_2-473–100, where 'Al_2O_3' and 'SiO_2' indicate the support, '473' reflects the reduction temperature in K, '100' means that 100 % hydrogen flow was used during reduction. Subscript numbers indicate the weight percentage of each metal.

Temperature-programmed desorption of water from initial γ-Al_2O_3 and SiO_2 supports showed that they contain ca. 4 and 3 H_2O molecules per nm^2, respectively (**Figure S1**, **Table S2**); pretreatment at 473 K leaves only 1–2 H_2O molecules per nm^2. As dehydration of SiO_2 at 673 K under inert gas leaves only about 0.3 H_2O molecules per nm^2, we decided to additionally test how this dehydration procedure performed right after the reduction impacts the catalytic activity of the SiO_2-supported catalyst ($Pt_{2.0}Fe_{1.4}$-SiO_2-473–100-deh). The $Pt_{2.0}Fe_{1.4}$-Al_2O_3-473–100-deh underwent self-reduction of iron during the dehydration process at 673 K (**Figure S9b**) and was consequently excluded from the current study.

The third set of samples (**Fig. 1a**) was prepared by adding water before or during the reduction pretreatment. $Pt_{2.1}Fe_{3.6}$-Al_2O_3-wet-473–100 and $Pt_{2.1}Fe_{3.6}$-Al_2O_3-wet-373–100 were impregnated with deionized water before the reduction (**Table S3**). The water volume was kept equal to the pore volume of the support. By dividing the volume of liquid water by the surface area of the support, we estimated that roughly 3400 H_2O molecules can be present for each nm^2 of the support surface, which clearly points to the existence of liquid water in the pores before reduction.

For the last set of samples (**Fig. 1a**), we tested how only adsorbed water affects the activity, $Pt_{2.1}Fe_{3.6}$-Al_2O_3-473–98-steam and $Pt_{2.0}$-

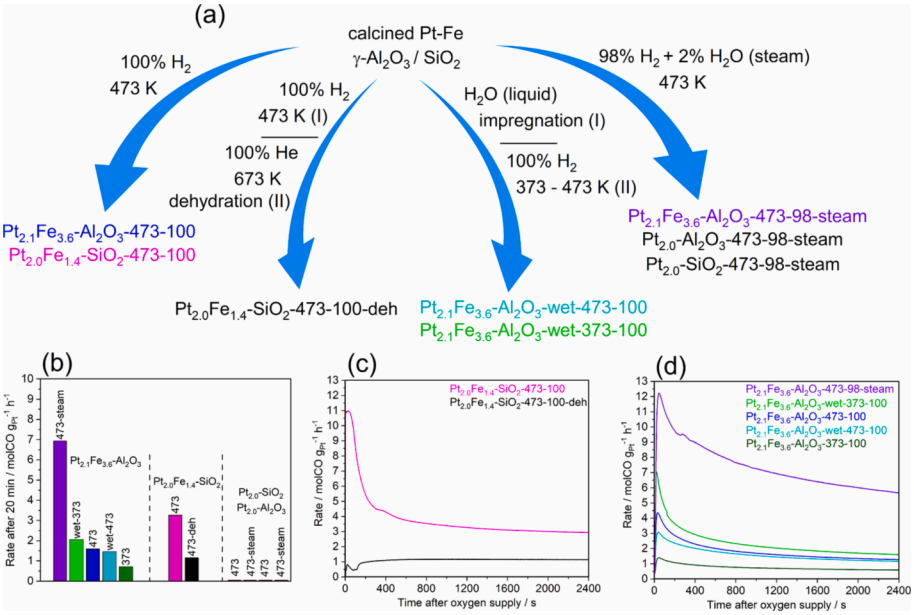

Fig. 1. Schematic representation of the preparation of specific catalysts explaining different pretreatment protocols (a). PROX activities of the catalysts under study after 20 min under PROX mixture (b). Time-on-stream PROX activities of SiO_2- (c) and γ-Al_2O_3-supported (d) catalysts under study. Reaction feed: 40 % H_2, 5 % CO, 2 % O_2, and helium balance. Reaction temperature 313 K. Sample names specify the samples compositions and the pre-treatment conditions typically involving reduction in concentrated hydrogen and several optional conditions, such as the impregnation of the samples with water (wet), the addition of water (2 %) into hydrogen flow during the reduction (steam) or an additional dehydration step in an inert gas at 673 K (deh).

Al_2O_3-473–98-steam were reduced under the gas mixture of 98 vol% H_2 and 2 vol% H_2O (Figure S2). The total amount of water added by the aforementioned steam treatment was estimated by the temperature programmed desorption to be around 4 H_2O molecules per nm^2 (Figure S1) for the pure γ-Al_2O_3 support, in addition to 1.2 H_2O molecules per nm^2 already present on the support surface at ambient temperature (Figure S1, Table S1). For all the experiments, water levels in the gas phase were measured by mass spectrometer using the signal of water (18 amu) normalized by the signal of helium (4 amu) (Figure S1**8**).

For each experiment, a fresh portion of the previously calcined catalyst from the same batch was placed in an operando reactor cell dedicated either to XAS or DRIFTS experiments. XAS experiments made use of the operando cell connected to our setup for preferential carbon monoxide oxidation shown in Figure S2 [26,28]. The same setup was used for operando DRIFTS measurements with the dedicated DRIFTS cell instead [28]. Each catalytic experiment started with the water-assisted or dry reduction, after which the catalyst was cooled to 313 K under helium or argon atmosphere and exposed to 40 vol% H_2 + 5 vol% CO for 10 min. Significant catalytic activity appeared after the addition of 2 vol% O_2 into the reaction mixture, as shown in Fig. 1**c,d**. During these experiments, selectivity to carbon monoxide oxidation for all catalysts at 313 K was above 99 %; only for $Pt_{2.1}Fe_{3.6}$-Al_2O_3-473–98-steam, it was above 97 %. During all operando experiments, carbon monoxide conversion was kept below 20 % to preserve a kinetically controlled regime of carbon monoxide oxidation.

As evident from Fig. 1**b-c**, the $Pt_{2.1}Fe_{3.6}$-Al_2O_3-473–98-steam outperforms all other catalysts in this study. In fact, it shows one of the highest reported preferential carbon monoxide oxidation activities among Pt-Fe catalysts on inert supports reported in literature (Table S3). The activity of $Pt_{2.1}Fe_{3.6}$-Al_2O_3-473–98-steam after 20 min on stream (6.93 molCO $gPt^{-1}h^{-1}$, Fig. 1**b**) is slightly higher than that of the state-of-the-art catalysts comprised of iron hydroxides supported on platinum nanoparticles by atomic layer deposition (5.61 molCO $gPt^{-1}h^{-1}$, Fig. 1**b**) [29]. Notably, only more complex catalytic materials, such as Pt/FeNi$(OH)_x$/TiO_2 and gold-based compositions in the presence of water vapor demonstrated higher activities per mass of noble metal (Table S3) [30]. An additional stability test performed under a simulated reformate feed: 5 vol% CO + 40 vol% H_2 + 10 vol% O_2 + 2 vol% H_2O / He confirms that $Pt_{2.1}Fe_{3.6}$-Al_2O_3-473–98-steam (15.5 molCO $gPt^{-1}h^{-1}$, Figure S3) outperforms the most active bimetallic Pt-Fe catalysts reported to date, obtained by Lou et al. with a solution deposition method (Table S3) [33]. Selectivity to carbon monoxide oxidation for $Pt_{2.1}Fe_{3.6}$-Al_2O_3-473–98-steam reaches only 65 % at 10 vol% O_2 and can be improved by decreasing the oxygen concentration.

Impregnation of bimetallic catalysts with water before the reduction step also has a significant promotion effect on the catalytic activity, but only if the reduction step is carried out at 373 K (Fig. 1**b,d**). The PROX reaction rate of $Pt_{2.1}Fe_{3.6}$-Al_2O_3-wet-373–100 after 20 min under PROX is 2.03 molCO $gPt^{-1}h^{-1}$, which is higher than for $Pt_{2.1}Fe_{3.6}$-Al_2O_3-473–100 (1.60 molCO $gPt^{-1}h^{-1}$) and $Pt_{2.1}Fe_{3.6}$-Al_2O_3-wet-473–100 (1.45 molCO $gPt^{-1}h^{-1}$). Interestingly, the reduction at 373 K without added water results in $Pt_{2.1}Fe_{3.6}$-Al_2O_3-373–100 with a significantly smaller PROX reaction rate of 0.7 molCO $gPt^{-1}h^{-1}$ (Fig. 1**b,d**). Addition of water during the reduction step evidently improves the PROX activity without compromising the carbon monoxide selectivity under the kinetic reaction regime. Catalyst dehydration significantly decreases the catalytic activity, for instance, $Pt_{2.0}Fe_{1.4}$-SiO_2-473–100 loses its activity after dehydration at 673 K under an inert atmosphere, as shown in Fig. 1**b,c**. After 20 min of the reaction, $Pt_{2.0}Fe_{1.4}$-SiO_2-473–100 shows a PROX reaction rate of 3.3 molCO $gPt^{-1}h^{-1}$; the dehydration at 673 K decreases this value to 1.16 molCO $gPt^{-1}h^{-1}$ for $Pt_{2.0}Fe_{1.4}$-SiO_2-473–100-deh (Fig. 1**b,c**). Reaction rates drop significantly over 20 min on stream for all catalysts except for deactivated $Pt_{2.0}Fe_{1.4}$-SiO_2-473–100-deh. This deactivation can plausibly be explained by dehydroxylation of active $FeO_x(OH)_y$ sites, which is irreversible under preferential carbon monoxide oxidation conditions. The activity of unpromoted platinum catalysts: $Pt_{2.0}$-Al_2O_3-473–100 and $Pt_{2.0}$-SiO_2-473–100 at 313 lies below the detection limit of the mass spectrometer (Fig. 1**b**).

2.2. Encapsulation of platinum nanoparticles

As evident from electron microscopy images, the addition of water

during reductive pretreatments does not significantly affect particle size distribution of the reduced alumina-supported catalysts, demonstrating nanoparticles of around 1–2 nm in size. Ex situ scanning transmission electron microscopy (STEM) coupled with energy dispersive X-ray emission spectroscopy analysis showed that the nanoparticles formed after reduction contain both iron and platinum (Figure S4). Reductive pretreatments without addition of water result in similar dispersions of platinum nanoparticles estimated by STEM and carbon monoxide chemisorption; the difference is only about 10–20 %. (Figure S5, Table 1). For water- and steam-treated materials, the situation is very different: the dispersion of platinum calculated from carbon monoxide chemisorption (Table 1) is significantly smaller (by a factor of 3–4) in comparison to the corresponding values estimated by STEM. This observed discrepancy suggests partial encapsulation of platinum nanoparticles with iron-containing phases. Similar effects were observed for supported metal nanoparticles demostrating of strong metal-support interaction [17,18,32]. It should be mentioned that Pt-Fe alloying during reduction up to 473 K was excluded by EXAFS, as shown in Figure S11 [26].

2.3. Influence of water on the reaction kinetics

Our results indicate that water likely assists the formation of a certain active FeO_x/Pt interface via overgrowth of Pt by some FeO_x or $FeO_x(OH)_y$ layer. To check the influence of water on the PROX activity of these catalysts, we added water vapor directly to the reaction feed. The exposure time to water was controlled using a mechanical 3-way valve (Figure S2). The water concentration added to the flow was varied between 0.8 and 2 vol% H_2O. Water content after the reactor was monitored using a mass spectrometer as indicated in Fig. 2. The appearance of water-related signals was delayed because of the strong water adsorption on the catalyst. The carbon monoxide oxidation rate increased with the water vapor addition and decreased upon its removal. This was tested repeatedly for various catalysts and yielded water reaction orders of 0.09–0.17 (Fig. 2**d**). The addition of water to the reaction stream for $Pt_{2.1}Fe_{3.6}$-Al_2O_3-473–100 and $Pt_{2.1}Fe_{3.6}$-Al_2O_3-wet-473–100 was realized after the main kinetic measurements (Fig. 2**a,c**), while a separate experiment was done for $Pt_{2.1}Fe_{3.6}$-Al_2O_3-473–98-steam to test the reproducibility (Fig. 2**b**). The water–gas shift reaction with a mixture of 5 vol% CO + 2 vol% H_2O showed rates below 0.008 molCO $g_{Pt}^{-1}h^{-1}$ for alumina-supported catalysts and also for $Pt_{2.0}Fe_{1.4}$-SiO_2-473–100 (Figure S6), which is two orders of magnitude smaller than the actual PROX rate, suggesting that this reaction is improbable. The methanation reaction did not take place as no methane ($m/z = 15$) was detected in the mass spectrometer during all kinetic tests. Clearly, water affects either the PROX catalytic cycle or the number of active sites. Previously, we reported that the PROX activity of Pt-Fe-FeO_x/γ-Al_2O_3 reduced in pure hydrogen at 673 K was not affected by the addition of water. Taking all this information together, we propose that the effect of water vapor on the catalytic activity depends on the catalyst history which strongly affects the structure of active sites. In particular, the reduction in hydrogen atmosphere containing steam at 473 K (Fig. 1**b,c**) generates more catalytic active sites. An activity enhancement by addition of water into the PROX reaction stream at 313 K was observed, in comparison to the material reduced in the absence of water (Fig. 2). This suggests that not only the number of active sites can increase by the water-assisted hydrogen pretreatment but also their structure and reactivity can be different.

Table 1
Particle size and dispersion estimated from the particle size (D_{STEM}) together with the platinum dispersion measured by carbon monoxide chemisorption experiments (D_{CO}) for alumina-supported Pt-Fe and Pt catalysts.

Catalyst	Mean particle size / nm	D_{STEM}	D_{CO}
$Pt_{2.1}Fe_{3.6}$-Al_2O_3-473–100	1.5 ± 0.3	0.20	0.24
$Pt_{2.1}Fe_{3.6}$-Al_2O_3-473–98-steam	0.9 ± 0.3	0.49	0.12
$Pt_{2.1}Fe_{3.6}$-Al_2O_3-wet-473–100	1.3 ± 0.3	0.28	0.09
$Pt_{2.0}$-Al_2O_3-473–100	1.0 ± 0.2	0.65	0.56

2.4. ^{18}O-labeling experiments

To further understand the promoting effect both of the water-assisted pretreatment and direct water addition into the feed, we performed targeted experiments with ^{18}O-labeled water. In these experiments, initially-calcined $Pt_{2.1}Fe_{3.6}$-Al_2O_3 was impregnated with $H_2^{18}O$ instead of standard water and then exposed to the same reduction and reaction procedures as the original $Pt_{2.1}Fe_{3.6}$-Al_2O_3-wet-473–100 and $Pt_{2.1}Fe_{3.6}$-Al_2O_3-wet-373–100 catalysts. Figure S7**a** shows no evidence of ^{18}O-labeled oxygen, carbon monoxide, carbon dioxide, or even water under the catalytic conditions over $Pt_{2.1}Fe_{3.6}$-Al_2O_3-wet($H_2^{18}O$)-473–100 pretreated at 473 K. This behavior explains why $Pt_{2.1}Fe_{3.6}$-Al_2O_3-473–100 and $Pt_{2.1}Fe_{3.6}$-Al_2O_3-wet-473–100 demonstrate similar activities. This suggests that during the reduction at 473 K, adsorbed water species evaporate and therefore show no influence on the catalytic activity.

On the contrary, $Pt_{2.1}Fe_{3.6}$-Al_2O_3-wet($H_2^{18}O$)-373–100 pretreated at 373 K retains some $H_2^{18}O$ on the surface, which indicates that reduction at 373 K is unable to completely remove adsorbed water. Right after the addition of oxygen to the hydrogen and carbon monoxide mixture, this catalyst exhibits a prominent peak of $C^{16}O^{18}O$ (Fig. 3**a),** which does not appear during the blank experiment with the unlabeled water (Fig. 3**b**). It is essential that the $C^{16}O^{18}O$ signal appears only after the addition of unlabeled oxygen to the feed. The rate of isotopic exchange between $H_2^{18}O$ and unlabeled CO_2 is 10 times smaller than the reaction rate (Figure S7**c**). Notably, the signals of ^{18}O-labeled water and carbon dioxide gradually disappear with time. $Pt_{2.1}Fe_{3.6}$-Al_2O_3-wet-373–100 is also significantly more active than $Pt_{2.1}Fe_{3.6}$-Al_2O_3-473–100 and $Pt_{2.1}Fe_{3.6}$-Al_2O_3-473-wet-100, which suggests that water or hydroxyl species present at the $FeO_x(OH)_y$/Pt interface are associated with more active sites. This was confirmed by another experiment during which a pulse of $H_2^{18}O$ vapor was added directly into the PROX mixture over $Pt_{2.1}Fe_{3.6}$-Al_2O_3-473–100, and the catalyst immediately produced $C^{16}O^{18}O$ (Fig. 3**c**). The observed production of $C^{16}O^{18}O$ cannot be explained by an isotopic exchange between water and reaction gases, as confirmed by blank experiments shown in Figure S7 **and 3d**. Thus, water or active hydroxyls adsorbed next to active Fe^{2+} sites can be directly involved in the PROX catalytic cycle [3].

2.5. Operando Fe K-edge XAS

As it was shown in our previous work, the ambient temperature PROX activity of supported Pt-Fe catalysts is directly proportional to the number of oxidic Fe^{2+} species at the catalytic interface [26]. We, therefore, set out to verify how the water-assisted pretreatment affects the amount and the reactivity of these active sites or possible even generates new active sites. Operando XAS allowed us to extract this information by measuring Fe K-edge XAS spectra during all kinetic measurements and temperature-programmed reduction experiments (see Figure S8). We performed a linear combination fit using Fe^{2+} and Fe^{3+} references to determine the concentration of the different oxidic iron species. Fe K-edge XAS of FeO was used as a general Fe^{2+} reference for all catalysts. Fe^{3+} references were slightly different for each catalyst; they were measured on each individual catalyst after PROX tests followed by temperature-programmed oxidation up to 473 K, assuring complete oxidation of all Fe^{2+}. In fact, the active Fe^{2+} is oxidized within 1 min upon the removal of carbon monoxide from the PROX mixture at 313 K and no additional oxidation is observed after the temperature programmed oxidation (Figure S9**a**). This suggests that Fe^{2+} centers are stabilized by the neighboring platinum covered by carbon monoxide [26,27].

Using these references, a linear combination fit of Fe K-edge XANES spectra in the 7100–7160 eV range made it possible to extract the

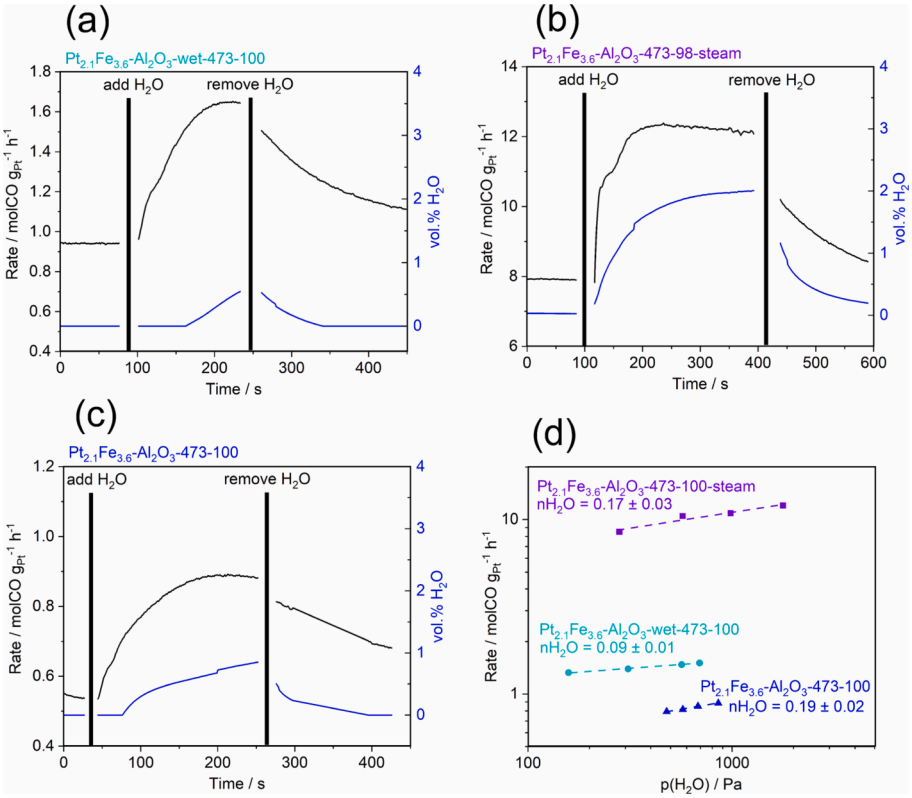

Fig. 2. The effect of the addition of water on the PROX rate at 313 K under 2 vol% O_2 + 40 vol% H_2 + 5 vol% CO at 313 K over $Pt_{2.1}Fe_{3.6}$-Al_2O_3-wet-473–100 (a), $Pt_{2.1}Fe_{3.6}$-Al_2O_3-473–98-steam (b), and $Pt_{2.1}Fe_{3.6}$-Al_2O_3-473–100 (c); correlations between the estimated partial pressure of added water and the PROX rate (d). nH_2O indicates water reaction order.

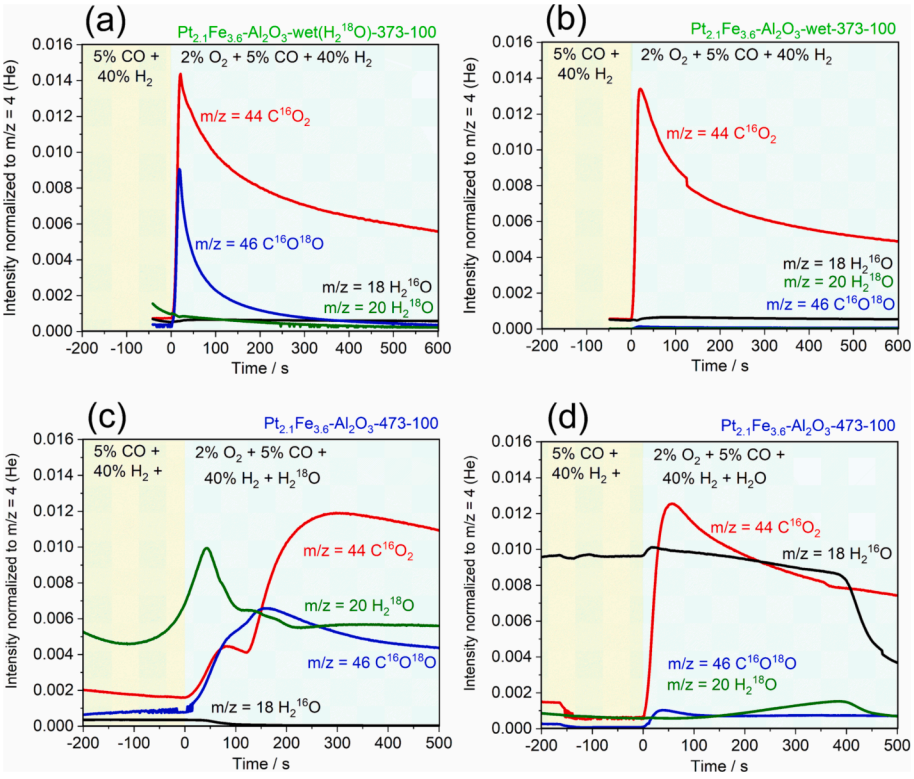

Fig. 3. Helium-normalized MS signals of reaction gases at 313 K during (a,b) oxygen addition into the PROX mixture over $Pt_{2.1}Fe_{3.6}$-Al_2O_3-wet-373–100 catalyst soaked with $H_2^{18}O$ before reduction (a) and soaked with standard water before reduction (b); helium-normalized MS signals of reaction gases at 313 K during direct addition of oxygen together with $H_2^{18}O$ (c) and standard H_2O (d) pulses over $Pt_{2.1}Fe_{3.6}$-Al_2O_3-473–100. Gas concentrations are shown in vol. %.

concentration of Fe^{2+} sites during temperature-programmed reduction, as shown in **Fig. 4a**. Metallic iron was not detected in any of the samples. About 44–46 % Fe^{2+} was formed after the reduction of $Pt_{2.1}Fe_{3.6}$-Al_2O_3-473–100 and $Pt_{2.1}Fe_{3.6}$-Al_2O_3-wet-473–100. As expected from the catalytic tests and experiments with $H_2^{18}O$, water desorbed below 473 K and, thus, had no effect on the amount of produced Fe^{2+}. However, water influenced the reduction of oxidic iron below 430 K, as shown in **Fig. 4a**. Moreover, for $Pt_{2.1}Fe_{3.6}$-Al_2O_3-473–98-steam catalyst, water vapor was constantly added during reduction, which promoted the formation of Fe^{2+}, resulting in ca. 54 % Fe^{2+}. The $Pt_{2.1}Fe_{3.6}$-Al_2O_3-wet-373–100 catalyst almost reproduced the iron reduction curve of $Pt_{2.1}Fe_{3.6}$-Al_2O_3-wet-473–100 below 373 K. The formation of iron hydroxides can facilitate Fe^{3+} reduction, as certain iron hydroxides are less thermodynamically stable towards reduction than iron oxides (**Table S4**). The Fe K-edge XANES and EXAFS spectra of $Pt_{2.0}Fe_{1.4}$-SiO_2-473–100 and $Pt_{2.0}Fe_{1.4}$-SiO_2-473–100-deh recorded after reduction are almost identical (**Fig. 4b**), which confirms that dehydration at 673 K does not change the local structure of the majority of iron species. Interestingly, iron sites in $Pt_{2.1}Fe_{3.6}$-Al_2O_3-473–100-deh sample undergo auto-reduction under helium at 673 K, similarly to FeZSM-5, which, however, does not affect the catalytic activity significantly (**Figure S9**) [34].

The Fe K-edge XANES data measured during 200–500 s of preferential carbon monoxide oxidation tests were averaged and shown in **Fig. 4c,d**. As we reported before, iron sites that can not be reduced by carbon monoxide are irreversibly oxidized during the first 100 s after the addition of oxygen, only the minority of sites remains in a reduced state under the steady-state conditions afterwards [26,27]. This explains why Fe K-edge XANES spectra of all catalysts under PROX look similar to fully oxidized ferrihydrite (4 Fe-O neighbours) or α-Fe_2O_3 (6 Fe-O neighbors) with only a tiny percentage of active Fe^{2+} sites. The Fe K-edge pre-edge position is sensitive to the oxidation state (**Figure S10**), while its increased intensity indicates a low number of close Fe-O neighbours [34,35]. This points to the low-coordinated nature of oligomeric oxidic surface iron species coordinating oxygen and water molecules in the catalyst [34,35]. Fourier-transformed Fe K-edge EXAFS spectra (**Figure S10**) show that the amplitude of the first Fe-O coordination sphere peak of Fe K-edge EXAFS at ca. 1.38 Å is the highest for $Pt_{2.1}Fe_{3.6}$-Al_2O_3-wet-373–100 and $Pt_{2.0}Fe_{1.4}$-SiO_2-473–100-deh.

As one can see in **Figure S10**, the second coordination shell peak at ca. 2.5 Å has an intermediate intensity between amorphous ferrihydrite (first Fe-O-Fe neighbor) and Fe_2O_3 for all catalysts. Fe K-edge EXAFS fitting (Fe-O 1.95 Å, Fe-O-Fe 2.94 Å) helped us to estimate aggregation and structure of these clusters. The best fit results are shown in **Table S5** and **Figs. S11-1 and S11-2**. For all catalysts, approximately 1–2 iron (Fe-O-Fe) neighbors were observed at a distance of about 2.94–2.96 Å (**Table S5**). The Fe-O coordination number for most samples is close to 4–5, which is typical for surface $FeO_x(OH)_y$ oligomers in a partially reduced state [26,27,29,35]. Smaller number of Fe-O-Fe bonds in $Pt_{2.1}Fe_{3.6}$-Al_2O_3-473–98-steam (**Table S5**) might indicate that water hinders the aggregation of oxidic iron clusters, while promoting the strong metal-support interaction.

A linear combination fit of Fe K-edge XANES allowed us to extract the average oxidation state of surface $FeO_x(OH)_y$ species. The results of these fits for the catalysts under PROX conditions in the time period of 200–500 s are presented in **Figure S12**; Fe K-edge XANES spectra were averaged every 100 s as shown in **Fig. 5a**. 54 % Fe^{2+} sites in $Pt_{2.1}Fe_{3.6}$-Al_2O_3-473–98-steam catalysts formed after reduction by hydrogen are rapidly oxidized under PROX conditions to 14–17 % Fe^{2+}; the same occurs for all alumina-supported catalysts, $Pt_{2.1}Fe_{3.6}$-Al_2O_3-473–100 and $Pt_{2.1}Fe_{3.6}$-Al_2O_3-wet-473–100 show similar amounts of Fe^{2+} sites (8–16 % Fe^{2+} under PROX conditions). The Fe^{2+} concentration in $Pt_{2.1}Fe_{3.6}$-Al_2O_3-wet-373–100 decreased to less than 2 % under PROX conditions.

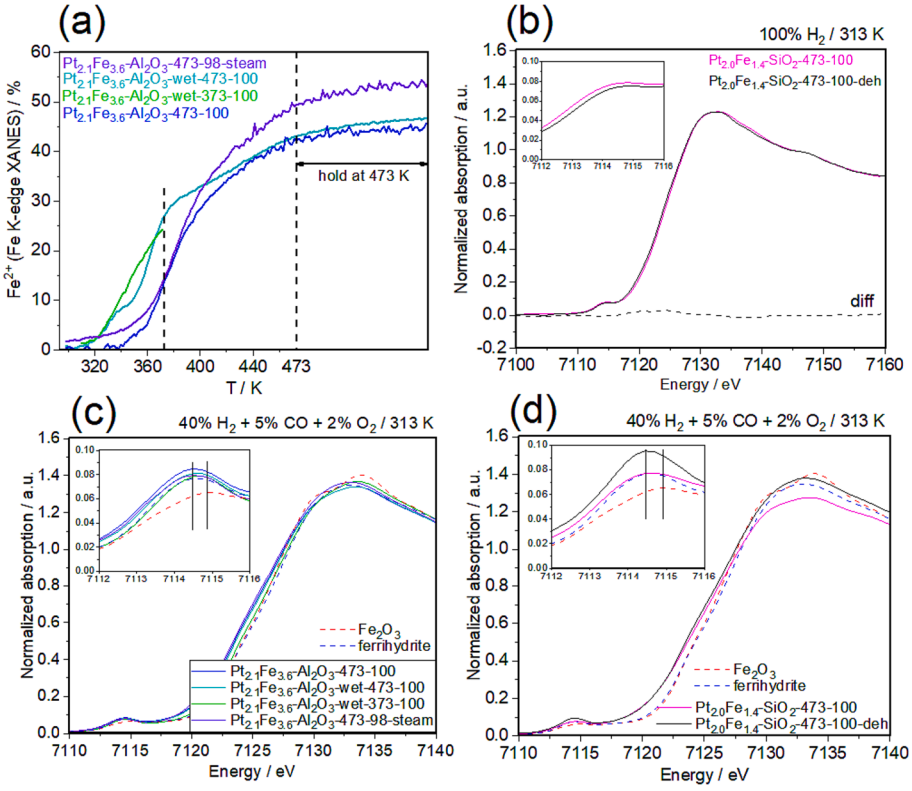

Fig. 4. Concentration of Fe^{2+} during the temperature-programmed reduction obtained using linear combination fitting of in situ Fe K-edge XANES (a); in situ Fe K-edge XANES of SiO_2-supported catalysts after reduction under 100 % H_2 and optional dehydration at 673 K under helium (b); operando Fe K-edge XANES of γ-Al_2O_3- (c) and SiO_2-supported (d) catalysts (solid lines) under PROX conditions at 313 K; Fe_2O_3, ferrihydrite references (dashed) are shown for comparison. Gas concentrations are shown in vol. %.

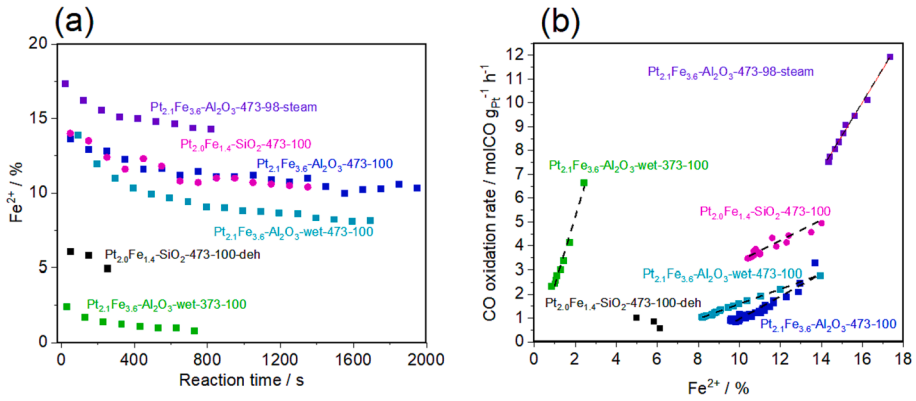

Fig. 5. Evolution of the Fe^{2+} concentration under PROX conditions for different catalysts monitored by operando Fe K-edge XANES (a). Correlation between the concentration of Fe^{2+} and the PROX activity (b). At time zero, we added 2 vol% O_2 into the 40 vol% H_2 + 5 vol% CO mixture; the reaction temperature was 313 K; data points were averaged every 100 s.

We correlated the PROX activity with the Fe^{2+} concentrations measured during the deactivation of the catalysts under PROX conditions (Fig. 5**b**). As we have shown in our previous work, the concentration of interface Fe^{2+} species linearly correlates with the PROX activity [26]. The slope between the PROX rate and Fe^{2+} concentration indicates how much carbon monoxide can be oxidized per single active Fe^{2+} cation. Water treatment, i.e. samples $Pt_{2.1}Fe_{3.6}$-Al_2O_3-473–98-steam and $Pt_{2.1}Fe_{3.6}$-Al_2O_3-wet-373–100, results in a steeper activity - Fe^{2+} concentration slope. This slope expressed in molCO ($molFe^{2+}$ s)$^{-1}$ units can be assigned to the apparent turnover frequency for each active Fe^{2+} site. For $Pt_{2.1}Fe_{3.6}$-Al_2O_3-wet-373–100, the slope is 2.5 molCO ($molFe^{2+}$ s)$^{-1}$; for $Pt_{2.1}Fe_{3.6}$-Al_2O_3-473–98-steam, it is 1.3 molCO ($molFe^{2+}$ s)$^{-1}$. As shown previously, $Pt_{2.1}Fe_{3.6}$-Al_2O_3-wet-473–100 does not retain any initially adsorbed water after the pretreatment step, thus, its slope is only 0.3 molCO ($molFe^{2+}$ s)$^{-1}$, which is close to 0.4 molCO ($molFe^{2+}$ s)$^{-1}$ observed for $Pt_{2.1}Fe_{3.6}$-Al_2O_3-473–100. $Pt_{2.0}Fe_{1.4}$-SiO_2-473–100 exhibits a slope of 0.8 molCO ($molFe^{2+}$ s)$^{-1}$. Further dehydration at 673 K under an inert atmosphere for $Pt_{2.0}Fe_{1.4}$-SiO_2-473–100-deh results in a lower number of active Fe^{2+} sites under PROX conditions as the Pt-$FeO_x(OH)_y$ interface is unstable without hydroxyl groups. The linear activity - Fe^{2+} trend of $Pt_{2.1}Fe_{3.6}$-Al_2O_3-473–98-steam does not reach zero. Most likely, along with the active Fe^{2+} sites, this catalyst contains a significant concentration of inactive (spectator) Fe^{2+}. The same is true for $Pt_{2.1}Fe_{3.6}$-Al_2O_3-473–100 and $Pt_{2.1}Fe_{3.6}$-Al_2O_3-wet-473–100. These spectator species most likely represent inactive or weakly active Fe^{2+} sites not accessible for direct oxidation and not participating in catalysis.

The oxygen reaction orders (Figure S13) during PROX are almost the same for all alumina-supported catalysts and lie within 0.7–0.8, which suggests that the presence of hydroxyl groups or adsorbed water on $Fe^{+2}O_x(OH)_y$ sites does not significantly influence the mechanism of oxygen activation over alumina-supported catalysts. At the same time, $Pt_{2.0}Fe_{1.4}$-SiO_2-473–100-deh has a lower oxygen reaction order (0.5), while the oxygen reaction order is much higher for $Pt_{2.0}Fe_{1.4}$-SiO_2-473–100 (1.0). Thus, we conclude that in the absence of iron-associated hydroxyl groups oxygen activation goes through the electrophilic oxygen species for the dehydrated $Pt_{2.0}Fe_{1.4}$-SiO_2-473–100-deh, as we have shown in our previous work [26]. At the same time, there is no clear correlation between water treatment and carbon monoxide reaction order, which always remains close to zero (Figure S13), suggesting the overall mechanism of carbon monoxide activation on platinum nanoparticles remains similar.

2.6. Operando DRIFTS experiments

In situ DRIFTS spectroscopy was subsequently employed to clarify the nature of adsorbed water and hydroxyl groups at the catalytic interface. For operando DRIFTS, we employed the same experimental protocols as for operando Fe K-edge XAS. Figure S14 shows averaged DRIFTS spectra of $Pt_{2.1}Fe_{3.6}$-Al_2O_3-473–100, $Pt_{2.0}$-Al_2O_3-473–98-steam, and $Pt_{2.1}Fe_{3.6}$-Al_2O_3-473–98-steam catalysts during 200–500 s of exposure to PROX conditions. Adsorbed water forms surface hydroxyl groups with the O–H stretching peaks centered at 3681 cm^{-1} for $Pt_{2.1}Fe_{3.6}$-Al_2O_3-473–98-steam and 3735 cm^{-1} for $Pt_{2.0}$-Al_2O_3-473–98-steam catalysts, respectively [24,25]. The C-O stretching vibration peak, corresponding to carbon monoxide linearly adsorbed on metallic platinum, shifts to lower wavenumbers for water-treated samples. $Pt_{2.1}Fe_{3.6}$-Al_2O_3-473–98-steam and $Pt_{2.0}$-Al_2O_3-473–98-steam exhibit these peaks at 2041–2042 cm^{-1}, while for $Pt_{2.1}Fe_{3.6}$-Al_2O_3-473–100, this peak is at 2052–2054 cm^{-1}. This shift indicates that water influences the electronic structure of platinum, [24,25] even for iron-free platinum-based catalysts. The shoulder at 2075 cm^{-1} is assigned to carbon monoxide adsorbed on $Pt^{\delta+}$ species; the band at 1820 cm^{-1} is typical for platinum nanoparticles of 1–2 nm in size [31]. Additional peaks at 1578 and 1457 cm^{-1} correspond to O-C-O stretching vibrations in carbonates and formates, which can form even in the absence of iron [25,36]. A broad band above 3650 cm^{-1} is present only for iron-containing samples and was previously observed for Pt-FeO_x catalysts exposed to carbon monoxide [25]. This band was found to be sensitive to the redox state of oxidic iron species and is likely associated with a change in reflectivity and a certain optical band gap of reduced iron oxide/hydroxide lattice [24,25].

Fast gas switching (reactants cut-off) experiments allowed us to extract the evolution of DRIFTS signals related to surface species involved in catalytic reaction. First, after 500 s exposure of $Pt_{2.1}Fe_{3.6}$-Al_2O_3-473–98-steam to PROX mixture, we cut all reactants using fast solenoid valves installed in our experimental setup (Figure S2) and replaced them with the same flow of argon. As evident from Fig. 6**a**, after the catalyst was left without any reactants, the intensity of the bands associated with surface –OH groups (3745 cm^{-1}) and adsorbed carbon monoxide (2058 cm^{-1}, 1842 cm^{-1}) decreased, and at the same time, the amount of adsorbed water increased as evident from the appearance of the bands at 2800–3300, 1637 and 1984 cm^{-1} [24,25]. A raise of the DRIFTS intensity at 1980 cm^{-1} indicates the change of surface carbon monoxide coverage [24,25]. The amount of produced gas phase carbon dioxide (2290–2390 cm^{-1}) initially increased and then gradually decreased [24,25]. This carbon dioxide should be produced from adsorbed carbon monoxide remaining on the platinum surface after the reactants cut-off. The integrated areas of each peak were normalized to the energy window (ΔE, cm^{-1}) are presented in Fig. 6**b**. From this figure, it can be deciphered that the consumption of carbon monoxide and hydroxyl groups happens simultaneously, as water-associated bands at 1598–1785 cm^{-1} and around 3000 cm^{-1} start appearing at the same time. The bands in the 1222–1596 cm^{-1} region corresponding to surface bicarbonates, carbonates, and formates cannot

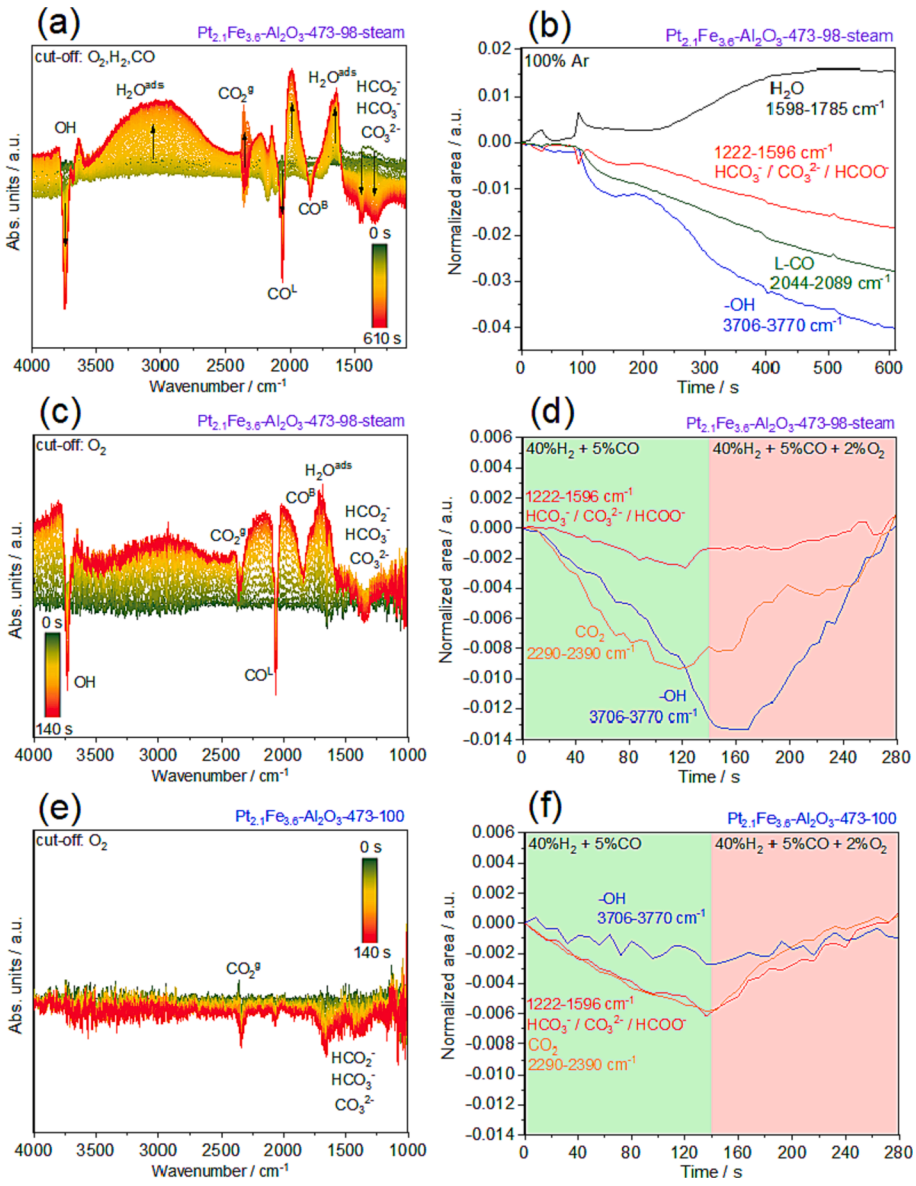

Fig. 6. In situ DRIFTS spectra measured during cut-off of all reactants over $Pt_{2.1}Fe_{3.6}$-Al_2O_3-473–98-steam (a) and cut-off of oxygen over $Pt_{2.1}Fe_{3.6}$-Al_2O_3-473–98-steam (c) and $Pt_{2.1}Fe_{3.6}$-Al_2O_3-473–100 (e); The corresponding changes in the normalized area of assigned DRIFTS peaks are shown on the right side (b, d, and f). All spectra were measured at 313 K; gas concentrations were 40 vol% H_2, 5 vol% CO, 2 vol% O_2.

be separated from each other and are likely related to the shift in DRIFTS background due to the change in surface reflectivity [36,37].

The results of oxygen cut-off experiments shown in Fig. 6**c,d** confirm that surface hydroxyl groups participate in the oxidation of carbon monoxide under reaction conditions over $Pt_{2.1}Fe_{3.6}$-Al_2O_3-473–98-steam. Hydroxyl groups (3730 cm^{-1}) are removed together with the gas phase carbon dioxide (2290–2390 cm^{-1}) immediately after the oxygen cut-off (Fig. 6**c**). These hydroxyl groups are absent for the $Pt_{2.1}Fe_{3.6}$-Al_2O_3-473–100 catalyst (Fig. 6**e**), which shows only a slight decrease in the carbon dioxide band intensity due to lower PROX activity. Surface bicarbonate, carbonate, and formate species do not play a significant role in PROX over $Pt_{2.1}Fe_{3.6}$-Al_2O_3-473–98-steam as evident from Fig. 6**d**, in contradiction to the previously proposed water-assisted mechanism involving surface formates (HCOO) [37]. As was shown previously for Pt-FeO_x/γ-Al_2O_3, these species are always present on the surface of the γ-Al_2O_3 support, and their formation does not limit the desorption of carbon dioxide as the reaction product [36]. The hydroxyl groups reacting with adsorbed carbon monoxide (Fig. 6**d**) are formed during oxygen exposure of $Pt_{2.1}Fe_{3.6}$-Al_2O_3-473–98-steam and are quickly consumed upon oxygen removal. The concentration of hydroxyl groups do not change during oxygen cut-off experiment over $Pt_{2.0}$-Al_2O_3-473–98-steam (**Figure S15**), which suggests that the reactive hydroxyl groups are linked exclusively to the interfacial iron sites and that the formation of surface hydroxylated $FeO_x(OH)_y$ species is responsible for the enhanced PROX activity.

2.7. *Active $FeO_x(OH)_y$/Pt interface*

All performed experiments strongly suggest that the presence of iron-associated hydroxyl groups is critical to ensure high activity in preferential carbon monoxide oxidation at ambient temperature. The complex synthetic methods reported earlier are not always necessary to create active interfacial Pt/$FeO_x(OH)_y$ sites. A simple treatment of supported Pt-Fe catalysts with water during the reduction in hydrogen at 473 K makes it possible to achieve one of the highest activities reported to date (**Table S3**). Moreover, the dehydration of platinum-iron catalysts at 673 K (as in the case of $Pt_{2.0}Fe_{1.4}$-SiO_2-473–100-deh) reduces the activity of the catalyst by an order of magnitude.

Importantly, the introduction of water during the reduction step below 473 K increases the apparent PROX turnover rate of active Fe^{2+} sites (Fig. 5**b**). Since the oxygen reaction order for the most active catalysts is close to unity (0.7–1.0) and the catalytic activity is proportional to the concentration of Fe^{2+} sites (reduced, hence not saturated with oxygen), we propose that the main rate-limiting step of ambient temperature PROX for the water-pretreated catalysts is the activation of oxygen (Scheme 1). As suggested by chemisorption measurements (Table 1) and Fe K-edge EXAFS, $FeO_x(OH)_y$ oligomers with about 1–2 nearest iron neighbors can partially cover the platinum surface. Since iron-associated hydroxyl groups distinguish the most active Pt-Fe catalysts, we could suggest two reaction mechanisms involving either dissociative or non-dissociative oxygen adsorption on unsaturated Fe^{2+} sites at the platinum interface. Dissociative oxygen adsorption would result in the following reaction pathway:

$$4Fe^{2+} + O_2 + 2H_2O \rightarrow 4(Fe^{3+} \bullet OH^-) \quad (1)$$

$$2(Fe^{3+} \bullet OH^-) + CO_{Pt} \rightarrow 2Fe^{2+} + CO_2 + H_2O \quad (2)$$

where CO_{Pt} represents a carbon monoxide molecule adsorbed on platinum.

Water-assisted carbon monoxide oxidation without the Fe^{2+}/Fe^{3+} redox cycle, as reported for Au-nanoparticles on various oxides, can also take place [38]. However, likely it is not the main mechanism of room-temperature-active Pt-Fe catalysts, since the active Fe^{2+} centers associated with high activity are only stable in the presence of carbon monoxide. As shown in Figure S9**a**, the removal of carbon monoxide from the PROX mixture at 313 K results in complete and irreversible (at 313 K) oxidation of these Fe^{2+} species within 1 min. This indicates high redox lability of active Fe^{2+} species and suggests their possible redox involvement in oxygen activation. Moreover, in our previous work, [26] we performed the transient oxygen cut-off experiments for room-temperature-active Pt-Fe catalysts with comparable structure and activity. These experiments have shown a slight but reversible increase in the concentration of Fe^{2+} while switching off the oxygen supply to the PROX mixture at 313 K, pointing at the possible involvement of Fe^{2+}/Fe^{3+} redox couple in the catalytic cycle.

As suggested in the literature, the presence of $FeO_x(OH)_y$ species enables to retain and rapidly exchange hydroxyl groups and water [29,30]. The presence of catalytically active hydroxyl groups is confirmed by DRIFTS (Fig. 6). However, as Eq. (1) suggests, the dissociative water-assisted adsorption of oxygen requires up to four iron atoms. The oxygen reaction orders of 0.7–1.0 better correspond to a non-dissociative mechanism of oxygen activation. The non-dissociative water-assisted adsorption of oxygen can be realized through OOH^- intermediates, as discovered previously for gold-based carbon monoxide oxidation catalysts [38]. In this case, another reaction pathway could take place:

$$2Fe^{2+} + O_2 + H_2O \rightarrow (Fe^{3+} \bullet OOH^-) + (Fe^{3+} \bullet OH^-) \quad (3)$$

$$(Fe^{3+} \bullet OOH^-) + (Fe^{3+} \bullet OH^-) + 2CO_{Pt} \rightarrow 2Fe^{2+} + 2CO_2 + H_2O \quad (4)$$

In both cases, oxygen activation is the limiting step, and hydroxyl groups are directly involved. Previous theoretical studies confirm that hydroxylation of oxidic iron species at the Pt - FeO_x interface can, indeed, decrease the reaction barrier of carbon monoxide oxidation [39,40]. Based on these findings, we propose the generalized mechanism drawn in Scheme 1. Importantly, individual hydrogen atoms are not spent in the catalytic cycle but must be permanently present on the surface in the form of adsorbed water or hydroxyl groups. The necessity of O_2 activation on multi-Fe^{2+} centers is considered in Scheme 1. However, since the average Fe-O-Fe coordination number obtained from EXAFS (Table S5) for the most active catalysts is close to unity, these centers are likely to be $Fe_nO_x(OH)_y$ oligomers.

An additional experiment with $Pt_{2.1}Fe_{3.6}$-Al_2O_3-wet-473–100 monitoring the concentration of Fe^{2+} using operando Fe K-edge XAS during the addition of water directly into the PROX mixture (Figure S16) shows that while added water increases the carbon monoxide oxidation rate, it does not affect the average oxidation state of iron. We believe that this happens because the addition of water at 313 K increases the turnover frequency of already existing active iron sites (being in their resting Fe^{2+} state) but does not create additional active sites or completely change the mechanism mainly determined by the nature of active Fe^{2+} species formed upon the catalyst pretreatment (Fig. 5**b**). In contrast, for Au-based room-temperature-active carbon monoxide oxidation catalysts operating by non-redox water-assisted mechanism, it was demonstrated [38] that promotion by water is mainly related to the increase in the number of Au sites activating oxygen. From this experiment, it is clear that water can influence the structure of active sites only at higher temperatures (e.g. 473 K). Fe K-edge EXAFS shows that $Pt_{2.1}Fe_{3.6}$-Al_2O_3-473–98-steam contains $FeO_x(OH)_y$ species in the least aggregated state (~0.7 Fe-O-Fe neighbors, Table S5) in comparison to other samples. This is consistent with the chemisorption measurements and confirms that $FeO_x(OH)_y$ species formed during steam – hydrogen pretreatment partially encapsulate platinum nanoparticles. Water treatment might stabilize active $FeO_x(OH)_y$ species at the platinum interface by

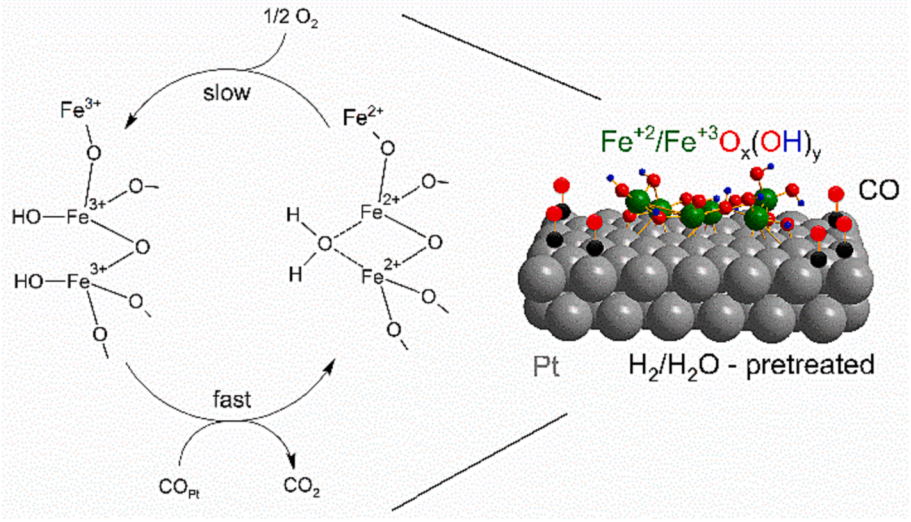

Scheme 1. Schematic representation of the proposed mechanism of preferential carbon monoxide oxidation over catalytically active $FeO_x(OH)_y$/Pt sites. The model of the $FeO_x(OH)_y$/Pt interface optimized by DFT is presented on the right.

promoting the strong metal-support interaction between platinum and iron and preventing their aggregation in an inactive Fe_2O_3-like phase proposed before [26]. At the same time, an additional iron neighbor would be required to retain surface hydroxyl groups and water as shown in **Scheme 1**.

To prove that water treatment at high temperatures can stabilize $FeO_x(OH)_y$ oligomers on the surface of metallic platinum, we employed density functional theory calculations of an optimized model of $Fe_6O_{14}H_{11}$/Pt(1 1 1) depicted in **Scheme 5-1**. The calculations (**Figure S17**) showed that dehydration of this structure results in its destabilization with dE = +0.38 eV after the removal of three structural water molecules and dE = +0.94 after the removal of five water molecules. Thus, the insertion of water in the structure has a definitive stabilization effect and prevents oligomeric $FeO_x(OH)_y$ species from aggregation and irreversible oxidation, leading to higher PROX activities. Therefore, water is essential to stabilize the active catalytic $FeO_x(OH)_y$/Pt interface.

3. Conclusions

By means of a simple incipient wetness impregnation method, we prepared supported platinum-iron catalysts that are active in preferential carbon monoxide oxidation at ambient temperature. The reduction of alumina-supported platinum-iron catalysts under hydrogen mixed with water vapor allowed us to create one the most active oxidation bimetallic platinum-iron catalysts on inert supports reported to date. Operando XAS experiments demonstrated that water-treated platinum-iron catalysts supported on alumina exhibit PROX turnover frequencies of 1.3–2.5 molCO $(molFe^{2+}\ s)^{-1}$ for active Fe^{2+} sites, which is higher than for non-water treated catalysts exhibiting lower corresponding values of 0.3–0.4 molCO $(molFe^{2+}\ s)^{-1}$. We established that the addition of liquid water before the reduction pretreatment in pure hydrogen or the addition of steam in hydrogen during the pretreatment facilitates the reduction of surface iron oxidic oligomers and creates active $FeO_x(OH)_y$/Pt interface sites responsible for the enhanced PROX reaction rate. The formation of these $FeO_x(OH)_y$ sites correlates with the observed partial encapsulation of platinum nanoparticles, providing a new example of a positive role of strong metal-support interaction for the design of catalysts [17]. Direct addition of water vapor into the PROX steam at ambient temperature can also increase the catalytic activity by hydroxylating $FeO_x(OH)_y$ species but is unable to change the concentration and the structure of active Fe^{2+} sites. On the contrary, dehydration of platinum-iron catalysts decreases the number of active Fe^{2+} sites explaining the deactivation.

Funding sources

We would like to extend our gratitude to the Swiss National Science Foundation for funding this research (Project 200021_179132).

CRediT authorship contribution statement

Ilia I. Sadykov: Conceptualization, Data curation, Formal analysis, Investigation, Methodology, Software, Validation, Writing – original draft, Writing – review & editing. **Dennis Palagin:** Formal analysis, Investigation. **Frank Krumeich:** Investigation, Methodology. **Igor V. Plokhikh:** Investigation. **Jeroen A. van Bokhoven:** Supervision, Writing – review & editing. **Maarten Nachtegaal:** Writing – review & editing. **Olga V. Safonova:** Conceptualization, Funding acquisition, Project administration, Supervision, Writing – review & editing.

Declaration of competing interest

The authors declare the following financial interests/personal relationships which may be considered as potential competing interests: Olga V. Safonova reports financial support was provided by Swiss National Science Foundation.

Data availability

Data will be made available on request.

Acknowledgment

We thank Dr. Davide Ferri for providing the cell and his help during operando DRIFTS experiments. We are grateful to Dr. Alexey Fedorov and Evgenia Kountoupi for their help with chemisorption measurements. We thank Dr. Luca Artiglia and Xiansheng Li for the help with the XPS measurements. Many thanks to Prof. Dr. Gunnar Jeschke and Sergei Kuzin for the EPR measurements. We are grateful to the people who helped with operando experiments: Dr. Adam H. Clark, Dr. Miren Agote Arán, Dr. Anna Zabilska, Dr. Mikalai Artsiusheuski, Luca Maggiulli, Dr. Maneka Claire Roger, Filippo Buttignol, Jan Alfke, Patrick Gäumann, Sumant Phadke, and Lunhan Chen. The allocation of beamtime at the SuperXAS beamline at the Swiss Light Source is appreciatively acknowledged. The help of the Scientific Center for Optical and Electron Microscopy at ETH Zürich is gratefully acknowledged. The authors acknowledge the use of computational resources of DelftBlue supercomputer, provided by Delft High Performance Computing Centre.

Appendix A. Supplementary data

Supplementary data to this article can be found online at https://doi.org/10.1016/j.jcat.2023.115263.

References

[1] K. Liu, C. Song, V. Subramani (Eds.), Hydrogen and Syngas Production and Purification Technologies, John Wiley & Sons Inc, 2010, pp. 127–155.
[2] Ausfelder, F. and Bazzanella, A. Hydrogen in the chemical industry. In Hydrogen science and engineering: materials, processes, systems and technology, First Edition, in: D. Stolten, and B., Emonts, (Ed.), John Wiley & Sons, Inc., 2016; pp. 19-39.
[3] P.R. Davies, On the role of water in heterogeneous catalysis: a tribute to professor M. Wyn Roberts, Topics in Catal. 59 (2016) 671–677.
[4] G. Li, B. Wang, D.E. Resasco, Water-Mediated Heterogeneously Catalyzed Reactions, ACS Catal. 10 (2019) 1294–1309.
[5] C.R. Chang, Z.Q. Huang, J. Li, The promotional role of water in heterogeneous catalysis: mechanism insights from computational modeling, Wiley Interdisciplinary Rev.: Computational Molecular Sci. 6 (2016) 679–693.
[6] H.A. Al-Abadleh, V.H. Grassian, FT-IR study of water adsorption on aluminum oxide surfaces, Langmuir 19 (2003) 341–347.
[7] T. Morimoto, M. Nagao, J. Imai, The adsorption of water on SiO_2, Al_2O_3, and $SiO_2{\cdot}Al_2O_3$. The relation between the amounts of physisorbed and chemisorbed water, Bull. Chem. Soc. Japan 44 (1971) 1282–1288.
[8] W. Wang, H. Zhang, W. Wang, A. Zhao, B. Wang, J.G. Hou, Observation of water dissociation on nanometer-sized FeO islands grown on Pt (111), Chem. Phys. Let. 500 (2010) 76–81.
[9] F. Ringleb, Y. Fujimori, H.F. Wang, H. Ariga, E. Carrasco, M. Sterrer, H.J. Freund, L. Giordano, G. Pacchioni, J. Goniakowski, Interaction of water with FeO (111)/Pt (111): environmental effects and influence of oxygen, J. Phys. Chem. C 115 (2011) 19328–19335.
[10] L. Xu, Z. Wu, W. Zhang, Y. Jin, Q. Yuan, Y. Ma, W. Huang, Oxygen vacancy-induced novel low-temperature water splitting reactions on FeO (111) monolayer-thick film, J. Phys. Chem. C 116 (2012) 22921–22929.
[11] S. Gritschneder, M. Reichling, Structural elements of CeO2 (111) surfaces, Nanotech. 18 (4) (2006), 044024.
[12] A. Onsten, D. Stoltz, P. Palmgren, S. Yu, M. Gothelid, U.O. Karlsson, Water adsorption on ZnO (0001): Transition from triangular surface structures to a disordered hydroxyl terminated phase, J. Phys. Chem. C 114 (25) (2010) 11157–11161.
[13] F. Rohr, K. Wirth, J. Libuda, D. Cappus, M. Bäumer, H.J. Freund, Hydroxyl driven reconstruction of the polar NiO (111) surface, Surf. Sci. 315 (1–2) (1994) L977–L982.
[14] K. Persson, L.D. Pfefferle, W. Schwartz, A. Ersson, S.G. Järås, Stability of palladium-based catalysts during catalytic combustion of methane: The influence of water, Appl. Catal. b: Envir. 74 (3–4) (2007) 242–250.
[15] X. Li, X. Wang, I.I. Sadykov, D. Palagin, O.V. Safonova, J. Li, A. Beck, F. Krumeich, J.A. van Bokhoven, L. Artiglia, Temperature and reaction environment influence the nature of platinum species supported on ceria, ACS Catal. 11 (2021) 13041–13049.

[16] A.W. Petrov, D. Ferri, F. Krumeich, M. Nachtegaal, J.A. van Bokhoven, O. Kröcher, Stable complete methane oxidation over palladium based zeolite catalysts, Nature Comm. 9 (2018) 2545.
[17] T. Pu, W. Zhang, M. Zhu, Engineering Heterogeneous Catalysis with Strong Metal-Support Interactions: Characterization, Theory and Manipulation, Angew. Chem. Int. Ed. 62 (2023), e202212278.
[18] K.M. Siniard, M. Li, S.Z. Yang, J. Zhang, F. Polo-Garzon, Z. Wu, Z. Yang, S. Dai, Ultrasonication-Induced Strong Metal-Support Interaction Construction in Water Towards Enhanced Catalysis, Angew. Chem. (2023), e202214322.
[19] X. Li, X. Wang, I.I. Sadykov, D. Palagin, O.V. Safonova, J. Li, A. Beck, F. Krumeich, J.A. Van Bokhoven, L. Artiglia, Temperature and reaction environment influence the nature of platinum species supported on ceria, ACS Catal. 11 (21) (2021) 13041–13049.
[20] H. Frey, A. Beck, X. Huang, J.A. van Bokhoven, M.G. Willinger, Dynamic interplay between metal nanoparticles and oxide support under redox conditions, Science 376 (2022) 982–987.
[21] J. Knudsen, L.R. Merte, L.C. Grabow, F.M. Eichhorn, S. Porsgaard, H. Zeuthen, R. T. Vang, E. Lægsgaard, M. Mavrikakis, F. Besenbacher, Reduction of FeO/Pt (111) thin films by exposure to atomic hydrogen, Surf. Sci. 604 (2010) 11–20.
[22] H. Muraki, S.I. Matunaga, H. Shinjoh, M.S. Wainwright, D.L. Trimm, The effect of steam and hydrogen in promoting the oxidation of carbon monoxide over a platinum on alumina catalyst, J. Chem. Tech. & Biotech. 52 (1991) 415–424.
[23] M.M. Schubert, Mechanistic Insights into the Preferential CO Oxidation in H2-rich Gas (PROX) over Supported Noble Metal Catalysts, University of Ulm, 2000. PhD Thesis.
[24] S. Li, M. Jia, J. Gao, P. Wu, M. Yang, S. Huang, X. Dou, Y. Yang, W. Zhang, Infrared studies of the promoting role of water on the reactivity of Pt/FeO_x catalyst in low-temperature oxidation of carbon monoxide, J. Phys. Chem. C 119 (2015) 2483–2490.
[25] B. Zheng, G. Liu, L. Geng, J. Cui, S. Wu, P. Wu, M. Jia, W. Yan, W. Zhang, Role of the FeO_x support in constructing high-performance Pt/FeO_x catalysts for low-temperature CO oxidation, Catal. Sci. & Tech. 6 (2016) 1546–1554.
[26] I.I. Sadykov, V.L. Sushkevich, F. Krumeich, R.J.G. Nuguid, J.A. van Bokhoven, M. Nachtegaal, O.V. Safonova, Platinum-Iron(II) oxide sites directly responsible for preferential carbon monoxide oxidation at ambient temperature: an operando X-ray absorption spectroscopy study, Angew. Chem. Int. Ed. 135 (2023) e2022140.
[27] I.I. Sadykov, M. Zabilskiy, A.H. Clark, F. Krumeich, V.L. Sushkevich, J.A. van Bokhoven, M. Nachtegaal, O.V. Safonova, Time-resolved XAS provides direct evidence for oxygen activation on cationic iron in a bimetallic Pt-FeO_x/Al_2O_3 catalyst, ACS Catal. 11 (2021) 11793–11805.
[28] G.L. Chiarello, M. Nachtegaal, V. Marchionni, L. Quaroni, D. Ferri, Adding diffuse reflectance infrared Fourier transform spectroscopy capability to extended x-ray-absorption fine structure in a new cell to study solid catalysts in combination with a modulation approach, Rev. Sci. Instrum. 85 (2014), 074102.
[29] L. Cao, W. Liu, Q. Luo, R. Yin, B. Wang, J. Weissenrieder, M. Soldemo, H. Yan, Y. Lin, Z. Sun, C. Ma, Atomically dispersed iron hydroxide anchored on Pt for preferential oxidation of CO in H_2, Nature 565 (2019) 631–635.
[30] G. Chen, Y. Zhao, G. Fu, P.N. Duchesne, L. Gu, Y. Zheng, X. Weng, M. Chen, P. Zhang, C.W. Pao, J.F. Lee, Interfacial effects in iron-nickel hydroxide-platinum nanoparticles enhance catalytic oxidation, Science 344 (2014) 495–499.
[31] Y. Lou, J. Liu, A highly active Pt-Fe/γ-Al_2O_3 catalyst for preferential oxidation of CO in excess of H_2 with a wide operation temperature window, Chem. Comm. 53 (2017) 9020–9023.
[32] M.G. Willinger, W. Zhang, O. Bondarchuk, S. Shaikhutdinov, H.J. Freund, R. Schlögl, A case of strong metal–support interactions: combining advanced microscopy and model systems to elucidate the atomic structure of interfaces, Angew. Chem. Int. Ed. 53 (23) (2014) 5998–6001.
[33] J. Pérez-Ramírez, G. Mul, F. Kapteijn, J.A. Moulijn, A.R. Overweg, A. Doménech, A. Ribera, I.W.C.E. Arends, Physicochemical characterization of isomorphously substituted FeZSM-5 during activation, J. Catal. 207 (2002) 113–126.
[34] T. Hiemstra, Surface and mineral structure of ferrihydrite, Geochimica Et Cosmochimica Acta 105 (2013) 316–325.
[35] A. Tomita, T. Miki, T. Tango, T. Murakami, H. Nakagawa, Y. Tai, Fe K-Edge X-ray absorption fine structure determination of γ-Al2O3-Supported Iron-Oxide Species, ChemPhysChem 16 (2015) 2015–2020.
[36] A. Tomita, K.I. Shimizu, K. Kato, T. Akita, Y. Tai, Mechanism of low-temperature CO oxidation on Pt/Fe-containing alumina catalysts pretreated with water, J. Phys. Chem. C 117 (2013) 1268–1277.
[37] K.I. Tanaka, H. He, M. Shou, X. Shi, Mechanism of highly selective low temperature PROX reaction of CO in H_2: oxidation of CO via HCOO with OH, Catal. Today 175 (2011) 467–470.
[38] J. Saavedra, C.J. Pursell, B.D. Chandler, CO oxidation kinetics over Au/TiO_2 and Au/Al_2O_3 catalysts: evidence for a common water-assisted mechanism, JACS 140 (2018) 3712–3723.
[39] Y. Zhao, G. Chen, N. Zheng, G. Fu, Mechanisms for CO oxidation on Fe(III)-OH-Pt interface: a DFT study, Faraday Discuss. 176 (2014) 381–392.
[40] X. Gu, R. Ouyang, D. Sun, H. Su, W. Li, CO oxidation at the perimeters of an FeO/Pt (111) interface and how water promotes the activity: a first-principles study, ChemSusChem 5 (2012) 871–878.